

# FDTD Analysis of All-Dielectric Planar Chiral Metamaterials with Large Optical Activity

Yuu Wakabayashi, Junji Yamauchi, and Hisamatsu Nakano  
Faculty of Engineering, Hosei University  
3-7-2 Kajino-cho, Koganei, Tokyo 184-8584 Japan,  
e-mail: yuu.wakabayashi.66@gs-eng.hosei.ac.jp

## 1. Introduction

Artificially chiral planar nanostructures, often referred to as planar chiral metamaterials (PCMs), have invoked much interest due to their intriguing optical activity [1]-[4]. An array of gammadion-shaped nanoparticles is one of the promising candidates. Although the optical activity of PCMs composed of metallic structures is enhanced by surface plasmon resonances, such resonances are accompanied with loss. To resolve this problem, recent attention is also directed towards PCMs composed of dielectric materials [3],[4]. In this article, we numerically investigate the optical activity of all-dielectric PCMs using the finite-difference time-domain (FDTD) method [5]. Our numerical results are in good agreement with the data obtained using the reformulated Fourier modal method [4]. We next study a windmill-type PCM, which shows a bandwidth larger than the gammadion-type. In addition to the PCMs with  $C_4$  (fourfold rotational) symmetry, other types of planar nanostructures with  $C_2$  and  $C_1$  symmetries are also studied for comparison.

## 2. Gammadion-type PCM

We first study the characteristics of the gammadion-type PCM shown in Fig. 1. The configuration, classified as  $C_4$  symmetry with respect to the  $z$  axis, is exactly the same as that treated in Ref. [4], in which the configuration parameters are taken to be  $n_g = n_h = 3.0$ ,  $n_{\text{sub}} = 1.5$ , and  $t_g = t_h = 0.2 \mu\text{m}$ . The arm width and the spacing between the arms are chosen to be the same, i.e.,  $w = s = 0.08 \mu\text{m}$ . The periodicity of the particles is set to be  $\Lambda = 0.5 \mu\text{m}$ . Note that the reformulated Fourier modal method was employed in Ref. [4]. In this article, we adopt the FDTD method together with the periodic boundary condition, and confirm its effectiveness. The numerical parameters are chosen to be  $\Delta x = \Delta y = \Delta z = 0.01 \mu\text{m}$ . A linearly polarized ( $E_y$ ) plane wave is normally incident towards the  $+z$ -axis direction.

Figs. 2(a), (b) and (c), respectively, show the transmittance, polarization rotation angle  $\theta$ , and the ellipticity as a function of wavelength. The transmittance is expressed using a linearly polarized wave. The ellipticity angle  $\chi$  is defined as  $\tan\chi = (E_R - E_L) / (E_R + E_L)$ , where  $E_R$  and  $E_L$  are the components of the right- and left-hand circularly polarized waves, respectively. For a completely circularly polarized wave,  $\tan\chi = 1$ . As a reference, the data for a patch structure, in which all the gaps of the gammadion-type PCM are filled in, are also plotted by broken lines. In this case,  $\theta$  and  $\tan\chi$  are zero as expected.

Our results obtained with the FDTD method are in good agreement with the published data, confirming the validity of our computer code. It has been suggested in Ref. [4] that the spectra in Fig. 2 are clearly divided into two regions (I and II) with respect to wavelength  $\lambda$ . In region I, both the polarization rotation and elliptization take place, whereas, in region II, the ellipticity  $\tan\chi$  is zero regardless of the polarization rotation. The division point between the two regions corresponds to  $\lambda_0 = n_{\text{sub}}\Lambda = 0.75 \mu\text{m}$ , beyond which no high-order diffraction would occur in the transmission region. We should also note that there is no polarization rotation in the reflected field.

### 3. Windmill-type PCM

Since the validity of our computer code has been confirmed, we next consider the modified (windmill-type) PCM shown in Fig. 3. The difference between the two PCMs lies in a 2D geometrical pattern. The basic configuration parameters are the same as those in the gammadion-type treated in the previous section, except for  $t_h = 0.16 \mu\text{m}$ . Other geometrical parameters are  $w = 0.06\sqrt{2} \mu\text{m}$ ,  $l_1 = 0.09\sqrt{2} \mu\text{m}$ , and  $l_2 = 0.14\sqrt{2} \mu\text{m}$ . The analysis is carried out under the same condition as that in the gammadion-type PCM.

Fig. 4 shows the data corresponding to Fig. 2. As in Fig. 2, there are two distinct regions in the spectra. In region II, we only have pure linear polarization rotation with the ellipticity being almost zero. At  $\lambda = 0.79 \mu\text{m}$ ,  $0.83 \mu\text{m}$ , and  $0.88 \mu\text{m}$  the incident  $y$ -polarized field is converted into the  $x$ -polarized field, as a half-wave plate does. It is interesting to note that this polarization rotation is not sensitive to wavelength, in comparison with that observed in Fig. 2. This leads to the alleviation of the fabrication accuracy. It should be noted at  $\lambda = 0.83 \mu\text{m}$  that the maximum transmittance is more than 0.85, which is higher than that obtained in Fig. 2(a). Fig. 4 also shows that 45-degree polarization rotation is obtained at  $\lambda \approx 0.85 \mu\text{m}$ . In region I, the conversion to a nearly circularly polarized wave is observed at several wavelengths, as a quarter-wave plate does. For example, at  $\lambda = 0.54 \mu\text{m}$ ,  $0.56 \mu\text{m}$ ,  $0.63 \mu\text{m}$ , and  $0.67 \mu\text{m}$ , the ellipticity exhibits a value of more than 0.7, although the transmittance remains relatively low.

### 4. PCMs with $C_2$ and $C_1$ Symmetries

So far we have treated the PCMs with  $C_4$  symmetry. We finally study the characteristics of nanostructures with  $C_2$  and  $C_1$  symmetries. The configurations are illustrated in Figs. 5 and 7. For the  $C_2$  symmetry case, a pair of gaps between the arms in the gammadion-type PCM is filled in, while for the  $C_1$  symmetry case, three gaps are filled in. The periodicity of the particles  $\Lambda$  is fixed to be the same as those for the PCMs with  $C_4$  symmetry, and the same dielectric materials are used. Other geometrical parameters are chosen to be  $w = s = 0.08 \mu\text{m}$ ,  $d = 0.16 \mu\text{m}$ , and  $t_h = 0.2 \mu\text{m}$ .

The transmittance and polarization spectra are shown in Fig. 6 and Fig. 8. It is found that the structures with  $C_2$  and  $C_1$  symmetries have only one polarization type, i.e., the region II disappears, which is observed at longer wavelengths in Fig. 2 and Fig. 4. Although 90-degree polarization rotation is obtained at some specific wavelengths, the rotation is not purely linearly polarized. The polarization rotation due to the elliptization is observed at not only shorter wavelengths but also longer wavelengths. Further calculation shows that polarization rotation occurs even in the reflected field, contrary to that for the PCMs with  $C_4$  symmetry. As expected, as the gaps are filled in, the transmittance behavior approaches that observed for the patch structure plotted by broken lines.

### 5. Conclusions

The FDTD method has been employed to assess the wavelength response of transmission through all-dielectric planar nanostructures with  $C_4$  symmetry. After confirming the validity of our FDTD results in a gammadion-type PCM, we investigate a windmill-type PCM, which shows that the polarization rotation observed at longer wavelengths becomes somewhat insensitive to wavelength change. Further consideration is directed towards nanostructures with  $C_2$  and  $C_1$  symmetries. The arrays of particles, in which a pair of gaps between the arms in the gammadion-type PCM or three gaps is filled in, show that there is no pure linear polarization rotation region (the type-II rotation), in contrast to the PCMs with  $C_4$  symmetry.

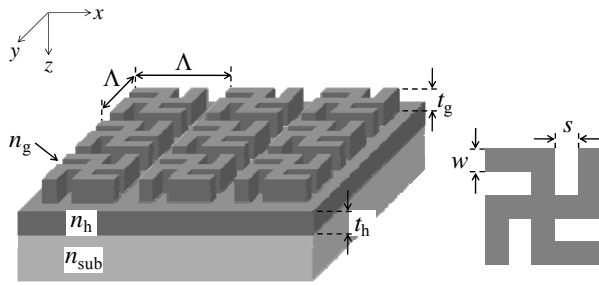


Fig. 1: Gammadion-type PCM

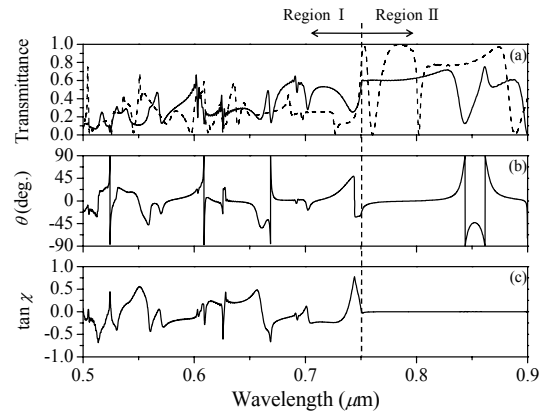


Fig. 2: Spectra of a gammadion-type PCM

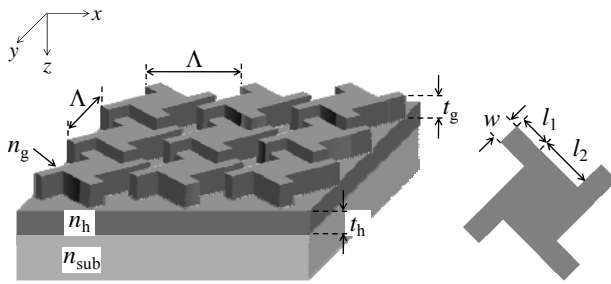


Fig. 3: Windmill-type PCM

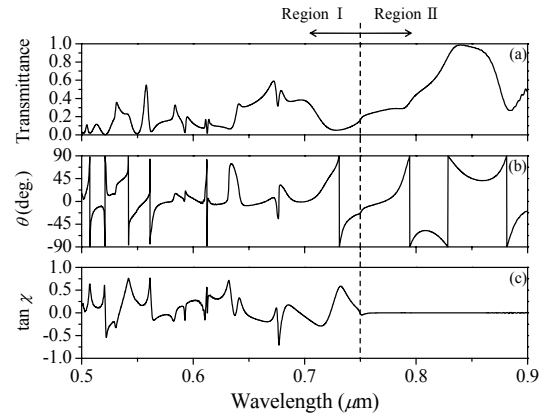


Fig. 4: Spectra of a windmill-type PCM

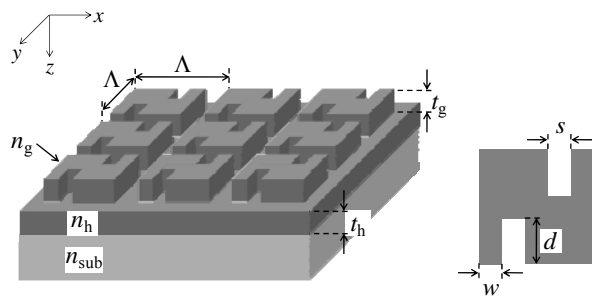


Fig. 5: PCM with  $C_2$  symmetry

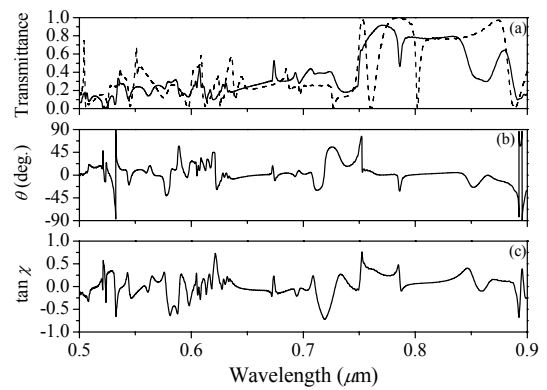


Fig. 6: Spectra of a PCM with  $C_2$  symmetry

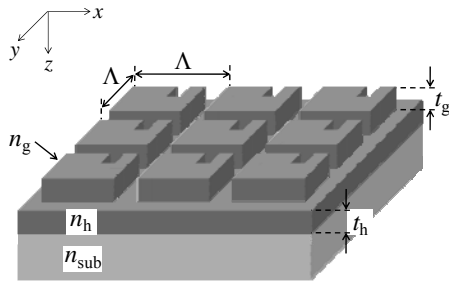


Fig. 7: PCM with  $C_1$  symmetry

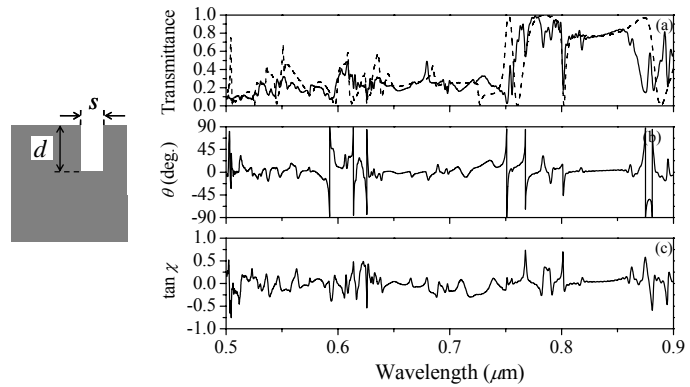


Fig. 8: Spectra of a PCM with  $C_1$  symmetry

## References

- [1] A. Papakostas, A. Potts, D. M. Bagnall, S. L. Prosvirnin, H. J. Coles, and N. I. Zheludev, "Optical manifestations of planar chirality," *Phys. Rev. Lett.*, vol. 90, 107404, Mar. 2003.
- [2] M. Kuwata-Gonokami, N. Saito, Y. Ino, M. Kauranen, K. Jefimovs, T. Vallius, J. Turunen, and Y. Svirko, "Giant optical activity in quasi-two-dimensional planar nanostructures," *Phys. Rev. Lett.*, vol. 95, 227401, Nov. 2005.
- [3] W. Zhang, A. Potts, and D. M. Bagnall, "Giant optical activity in dielectric planar metamaterials with two-dimensional chirality," *J. Opt. A. Pure Appl. Opt.*, vol. 8, pp. 878-890, Aug. 2006.
- [4] B. Bai, Y. Svirko, J. Turunen, and T. Vallius, "Optical activity in planar chiral metamaterial: Theoretical study," *Phys. Rev. A*, vol. 76, 023811, Aug. 2007.
- [5] A. Taflove and S. Hagness, *Computational Electrodynamics: The Finite-Difference Time-Domain Method*, 2nd edition, Boston: Artech House, 2000.